We are IntechOpen,
the world's leading publisher of
Open Access books
Built by scientists, for scientists

6,900
Open access books available

186,000
International authors and editors

200M
Downloads

Our authors are among the

154
Countries delivered to

TOP 1%
most cited scientists

12.2%
Contributors from top 500 universities

CLARIVATE ANALYTICS

BOOK CITATION INDEX

INDEXED

WEB OF SCIENCE™

Selection of our books indexed in the Book Citation Index
in Web of Science™ Core Collection (BKCI)

Interested in publishing with us?
Contact book.department@intechopen.com

Numbers displayed above are based on latest data collected.
For more information visit www.intechopen.com

No-Reflection Phenomena for Chiral Media

Yasuhiro Tamayama, Toshihiro Nakanishi,
Kazuhiko Sugiyama, and Masao Kitano
Department of Electronic Science and Engineering, Kyoto University
Japan

1. Introduction

Interest continues to grow in controlling the propagation of electromagnetic waves by utilizing periodically or randomly arranged artificial structures made of metal, dielectric, and other materials. When the size of the constituent structures and the separation between the neighboring structures are much smaller than the wavelength of the electromagnetic waves, the structure arrays behave as a continuous medium for the electromagnetic waves. That is, macroscopic medium parameters such as effective permittivity and permeability can be defined for the array. The artificial continuous medium is called a "metamaterial."

In the frequency region below the microwave frequency, the use of metallic structures as artificial media has been studied since the late 1940's (Collin, 1990). At first, only control of the permittivity was studied and not that of the permeability. However, Pendry et al. (1999) proposed methods for fabricating artificial magnetic media, namely, magnetic metamaterials, which were built from nonmagnetic conductors. It was shown that not only can relative permeability be changed from unity but it also can have a negative value. Although the relative permeabilities of naturally occurring media are almost unity in such high frequency regions as microwave, terahertz, and optical regions, the restriction that the relative permeability is almost unity can be removed using the metamaterial. Moreover, the magnetic metamaterial enabled us to fabricate media with simultaneous negative permittivity and permeability, or negative refractive index media that were predicted by Veselago (1968). In fact, Shelby et al. (2001) made the first experimental verification of a negative refractive index metamaterial in the microwave region. This increased researcher interest in metamaterials.

It was not possible to independently control the wavenumber and the wave impedance in a medium until magnetic metamaterials were developed. The wavenumber is related to the propagation and refraction of electromagnetic waves, and the wave impedance is connected with the reflection. Phenomena about electromagnetic waves are described by these two quantities. In dielectric media, both of the wavenumber and wave impedance change with a change of the permittivity, and we cannot set these parameters independently. However, the wavenumber and wave impedance can be changed independently in metamaterials because we can control the permeability as well as the permittivity with metamaterials. By utilizing the flexibility of the wavenumber and wave impedance in metamaterials, such novel phenomena as a perfect lens (superlens) (Pendry, 2000; Lagarkov & Kissel, 2004), a hyperlens (Jacob et al., 2006; Liu et al., 2007), and an invisibility cloak (Pendry et al., 2006; Leonhardt, 2006; Schurig et al., 2006) have been proposed and verified experimentally.

In this chapter, we focus on Brewster's no-reflection effect in metamaterials. The Brewster condition is one of the laws of reflection and refraction of electromagnetic waves at a boundary between two distinct media (Saleh & Teich, 2007). For a particular angle of incidence, known as the Brewster angle, the reflected wave vanishes. The Brewster effect is applied in optical instruments, for example, to generate completely polarized waves from unpolarized waves only with a glass plate and to suppress the insertion losses of intracavity elements.

The Brewster effect arises for transverse-magnetic (TM) waves [transverse-electric (TE) waves] at an interface between two distinct dielectric (magnetic) media. Hence, this phenomenon can only be observed for TM waves and not for TE waves in naturally occurring media that do not respond to high-frequency magnetic fields. However, since we can fabricate magnetic media in high frequency regions with a metamaterial technique (Pendry et al., 1999; Holloway et al., 2003; Zhang et al., 2005), the Brewster condition for TE waves can be satisfied (Doyle, 1980; Futterman, 1995; Fu et al., 2005). In fact, the TE Brewster effect has been experimentally observed in the microwave region (Tamayama et al., 2006) and also in the optical region (Watanabe et al., 2008).

In addition to permittivity and permeability, chirality parameter and non-reciprocity parameter can be controlled using metamaterials. It is also possible to control the anisotropy in electromagnetic responses. Therefore, investigating the no-reflection condition for generalized media is important. Brewster's condition has been studied for anisotropic media (Grzegorczyk et al., 2005; Tanaka et al., 2006; Shen et al., 2006; Shu et al., 2007), chiral media (bi-isotropic media) (Bassiri et al., 1988; Lindell et al., 1994), and bi-anisotropic media (Lakhtakia, 1992). However, thus far, the explicit relations among the medium parameters for achieving non-reflectivity in chiral and bi-anisotropic media have not been determined. The purpose of this chapter is to derive the explicit relation among the permittivity, permeability, and chirality parameter of the chiral medium that satisfy the no-reflection condition for a planar interface between a vacuum and the chiral medium.

The no-reflection condition is derived from the vanishing eigenvalue condition of the reflection Jones matrix. The analysis can be largely simplified by decomposing the reflection Jones matrix into the unit and Pauli matrices (Tamayama et al., 2008).

We find that in general chiral media, the no-reflection condition is satisfied by elliptically polarized incident waves for at most one particular angle of incidence. This is merely a natural extension of the usual Brewster effect for achiral (nonchiral) media. When the wave impedance and the absolute value of the wavenumber in the chiral medium equal those in a vacuum for one of the circularly polarized (CP) waves, the corresponding CP wave is transmitted to the medium without reflection for all angles of incidence. The no-reflection effect for chiral nihility media resembles that for achiral media.

We provide a finite-difference time-domain (FDTD) analysis (Taflove & Hagness, 2005) of the no-reflection effect for CP waves. We analyze the scatterings of electromagnetic waves by a cylinder and a triangular prism made of a chiral medium whose medium parameters satisfy the no-reflection condition for one of the CP waves. The simulation demonstrates that the corresponding CP wave is not scattered and the other CP wave is largely scattered. We show that a circular polarizing beam splitter can be achieved by utilizing the no-reflection effect.

2. Propagation of electromagnetic waves in chiral media

We calculate the wavenumber and wave impedance in chiral media. The constitutive equations for chiral media have several types of expressions. The Post and Tellegen representations are mainly used as the constitutive equations. The Post representation is

written as

$$D = \varepsilon_P E - i\xi_P B, \quad H = \mu_P^{-1} B - i\xi_P E, \tag{1}$$

and the Tellegen representation is written as

$$D = \varepsilon_T E - i\kappa_T H, \quad B = \mu_T H + i\kappa_T E, \tag{2}$$

where $\varepsilon_{P,T}$ is the permittivity, $\mu_{P,T}$ is the permeability, and ξ_P and κ_T are the chirality parameters. The subscript P (T) stands for the Post (Tellegen) representation. These representations are equivalent and interchangeable with the following transformation (Lakhtakia, 1992):

$$\varepsilon_T = \varepsilon_P + \mu_P \xi_P^2, \quad \mu_T = \mu_P, \quad \kappa_T = \mu_P \xi_P. \tag{3}$$

In this chapter, we consistently use the Post representation and omit the subscript P for simplicity.

Maxwell's equation for a monochromatic plane electromagnetic wave is given by

$$k \times E = \omega B, \quad k \times H = -\omega D, \tag{4}$$

where k is the wavenumber vector and ω is the angular frequency. Substituting Eq. (1) into Eq. (4) and assuming $k = k e_z$ (e_z is the unit vector in the z-direction), we obtain

$$
k \begin{bmatrix} 1 & & & O \\ & 1 & & \\ & & 1 & \\ O & & & 1 \end{bmatrix} \begin{bmatrix} E_x \\ E_y \\ H_x \\ H_y \end{bmatrix} = \omega \begin{bmatrix} 0 & i\mu\xi & 0 & \mu \\ -i\mu\xi & 0 & -\mu & 0 \\ 0 & -(\varepsilon + \mu\xi^2) & 0 & i\mu\xi \\ \varepsilon + \mu\xi^2 & 0 & -i\mu\xi & 0 \end{bmatrix} \begin{bmatrix} E_x \\ E_y \\ H_x \\ H_y \end{bmatrix}. \tag{5}
$$

From the condition for a non-trivial solution of Eq. (5), we have

$$k = \pm\omega(\sqrt{\varepsilon\mu + \mu^2\xi^2} + \mu\xi), \quad \pm\omega(\sqrt{\varepsilon\mu + \mu^2\xi^2} - \mu\xi). \tag{6}$$

After substitution of the derived wavenumber into Eq. (5), the relation among the wavenumber and the electromagnetic fields is obtained and summarized in Table 1. Here we define the wave impedance Z_c of the chiral medium as

$$Z_c = \sqrt{\frac{\mu}{\varepsilon + \mu\xi^2}}. \tag{7}$$

The eigenpolarizations in chiral media are found to be CP waves because $E_y/E_x = \pm i$ is satisfied.

Equations (6) and (7) contain double-valued square root functions. Thus, the wavenumber and wave impedance cannot be calculated without ambiguity. To choose the correct branch, we diagonalize Eq. (5). By using the transformation matrix

$$
U = \frac{1}{2} \begin{bmatrix} 1 & 1 & 1 & 1 \\ -i & i & i & -i \\ iZ_c^{-1} & iZ_c^{-1} & -iZ_c^{-1} & -iZ_c^{-1} \\ Z_c^{-1} & -Z_c^{-1} & Z_c^{-1} & -Z_c^{-1} \end{bmatrix}, \quad U^{-1} = \frac{1}{2} \begin{bmatrix} 1 & i & -iZ_c & Z_c \\ 1 & -i & -iZ_c & -Z_c \\ 1 & -i & iZ_c & Z_c \\ 1 & i & iZ_c & -Z_c \end{bmatrix}, \tag{8}
$$

k	k_+	$-k_+$	k_-	$-k_-$
E_x	1	1	1	1
E_y	$-i$	i	i	$-i$
H_x	iZ_c^{-1}	iZ_c^{-1}	$-iZ_c^{-1}$	$-iZ_c^{-1}$
H_y	Z_c^{-1}	$-Z_c^{-1}$	Z_c^{-1}	$-Z_c^{-1}$

Table 1. Relation among wavenumber and electromagnetic fields in chiral media. Ratio of each electromagnetic field component to E_x is written for each eigenmode. Here $k_\pm = \omega(\sqrt{\varepsilon\mu + \mu^2\xi^2} \pm \mu\xi) = \omega[Z_c(\varepsilon + \mu\xi^2) \pm \mu\xi]$ and $Z_c = \sqrt{\mu/(\varepsilon + \mu\xi^2)}$ [$\mathrm{Re}(Z_c) > 0$].

Eq. (5) is diagonalized as follows:

$$k\begin{bmatrix} E_x + iE_y - iZ_cH_x + Z_cH_y \\ E_x - iE_y - iZ_cH_x - Z_cH_y \\ E_x - iE_y + iZ_cH_x + Z_cH_y \\ E_x + iE_y + iZ_cH_x - Z_cH_y \end{bmatrix} = \begin{bmatrix} k_+ & & & O \\ & -k_+ & & \\ & & k_- & \\ O & & & -k_- \end{bmatrix} \begin{bmatrix} E_x + iE_y - iZ_cH_x + Z_cH_y \\ E_x - iE_y - iZ_cH_x - Z_cH_y \\ E_x - iE_y + iZ_cH_x + Z_cH_y \\ E_x + iE_y + iZ_cH_x - Z_cH_y \end{bmatrix}, \quad (9)$$

where we use the relation $Z_c(\varepsilon + \mu\xi^2) = \mu Z_c^{-1}$ [$Z_c^2 = \mu/(\varepsilon + \mu\xi^2)$] and set

$$k_\pm = \omega[Z_c(\varepsilon + \mu\xi^2) \pm \mu\xi]. \quad (10)$$

If Z_c is determined, $k_\pm$ can be calculated unambiguously. The real part of the wave impedance $\mathrm{Re}(Z_c)$ is related to the time-averaged Poynting vector, which governs the power flow of electromagnetic waves. When a branch of Z_c is chosen so that $\mathrm{Re}(Z_c) > 0$ is satisfied, the power flows of eigenmodes represented by the first and third (second and fourth) rows of Eq. (9) are directed to the positive (negative) z-direction. Thus, k_+ and k_- ($-k_+$ and $-k_-$) are the wavenumbers for the eigenmodes whose power flows are directed to the positive (negative) z-direction. Even if we choose a branch of Z_c that satisfies $\mathrm{Re}(Z_c) < 0$, we can obtain the same result by regarding $-Z_c$ as the wave impedance. Therefore, there is no loss of generality in supposing that the real part of Z_c is positive. The wavenumber and wave impedance can be calculated from Eqs. (7) and (10) and the condition $\mathrm{Re}(Z_c) > 0$ without ambiguity. We define the eigenmodes represented by the first and second (third and fourth) rows of Eq. (9) as left circularly polarized (LCP) [right circularly polarized (RCP)] waves.

3. Reflectivity and transmissivity for chiral media

We derive the reflectivity and transmissivity at the boundary between a vacuum and an isotropic chiral medium (Bassiri et al., 1988). As shown in Fig. 1, suppose that a monochromatic plane electromagnetic wave is incident from the vacuum (permittivity ε_0, permeability μ_0) on the chiral medium at an incident angle of θ. The electromagnetic fields of the incident (i), reflected (r), and transmitted (t) waves are written as follows:

$$\boldsymbol{E}_i = \boldsymbol{E}_1 \exp[ik_0(x\cos\theta - y\sin\theta)], \quad (11)$$

$$\boldsymbol{H}_i = \boldsymbol{H}_1 \exp[ik_0(x\cos\theta - y\sin\theta)], \quad (12)$$

$$\boldsymbol{E}_r = \boldsymbol{E}_2 \exp[ik_0(-x\cos\theta - y\sin\theta)], \quad (13)$$

$$\boldsymbol{H}_r = \boldsymbol{H}_2 \exp[ik_0(-x\cos\theta - y\sin\theta)], \quad (14)$$

$$\boldsymbol{E}_t = \boldsymbol{E}_3 \exp[ik_+(x\cos\theta_+ - y\sin\theta_+)] + \boldsymbol{E}_4 \exp[ik_-(x\cos\theta_- - y\sin\theta_-)], \quad (15)$$

$$\boldsymbol{H}_t = \boldsymbol{H}_3 \exp[ik_+(x\cos\theta_+ - y\sin\theta_+)] + \boldsymbol{H}_4 \exp[ik_-(x\cos\theta_- - y\sin\theta_-)], \quad (16)$$
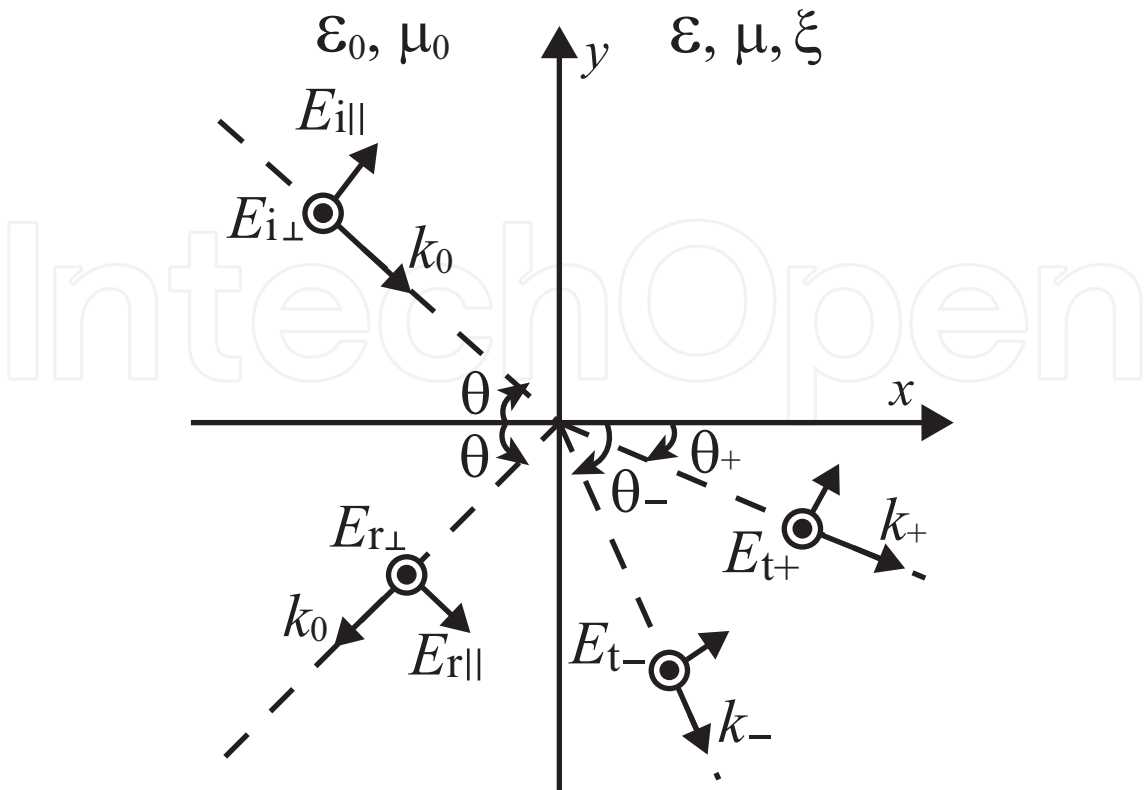
Fig. 1. Geometry of coordinate system. Incident, reflected, and transmitted waves are denoted by subscripts i, r, and t. Region $x < 0$ represents vacuum, and region $x \geq 0$ represents the chiral medium.

where

$$E_1 = E_{i\perp}e_z + E_{i\|}(\cos\theta e_y + \sin\theta e_x), \tag{17}$$

$$H_1 = Z_0^{-1}[E_{i\|}e_z - E_{i\perp}(\cos\theta e_y + \sin\theta e_x)], \tag{18}$$

$$E_2 = E_{r\perp}e_z + E_{r\|}(-\cos\theta e_y + \sin\theta e_x), \tag{19}$$

$$H_2 = Z_0^{-1}[E_{r\|}e_z + E_{r\perp}(\cos\theta e_y - \sin\theta e_x)], \tag{20}$$

$$E_3 = E_{t+}[i(\cos\theta_+ e_y + \sin\theta_+ e_x) + e_z], \tag{21}$$

$$H_3 = E_{t+}Z_c^{-1}[-(\cos\theta_+ e_y + \sin\theta_+ e_x) + ie_z], \tag{22}$$

$$E_4 = E_{t-}[-i(\cos\theta_- e_y + \sin\theta_- e_x) + e_z], \tag{23}$$

$$H_4 = E_{t-}Z_c^{-1}[-(\cos\theta_- e_y + \sin\theta_- e_x) - ie_z]. \tag{24}$$

In the above equations, $k_0 = \omega\sqrt{\varepsilon_0\mu_0}$ is the wavenumber in the vacuum, $Z_0 = \sqrt{\mu_0/\varepsilon_0}$ is the wave impedance of the vacuum, and e_x, e_y, and e_z are respectively the unit vectors in the x-, y-, and z-directions. Due to the translational invariance of the interface, Snell's equations

$$k_0\sin\theta = k_+\sin\theta_+ = k_-\sin\theta_-, \tag{25}$$

are satisfied. From the continuity of the tangential components of the electromagnetic fields across the boundary, we obtain

$$E_{i\perp} + E_{r\perp} = E_{t+} + E_{t-}, \tag{26}$$

$$E_{i\parallel}\cos\theta - E_{r\parallel}\cos\theta = iE_{t+}\cos\theta_+ - iE_{t-}\cos\theta_-, \tag{27}$$

$$Z_0^{-1}(E_{i\parallel} + E_{r\parallel}) = iZ_c^{-1}(E_{t+} - E_{t-}), \tag{28}$$

$$Z_0^{-1}(-E_{i\perp}\cos\theta + E_{r\perp}\cos\theta) = -Z_c^{-1}(E_{t+}\cos\theta_+ + E_{t-}\cos\theta_-). \tag{29}$$

The reflection and transmission matrices are derived from Eqs. (26)-(29) and written as

$$\begin{bmatrix} E_{r\perp} \\ E_{r\parallel} \end{bmatrix} = \begin{bmatrix} R_{11} & R_{12} \\ R_{21} & R_{22} \end{bmatrix} \begin{bmatrix} E_{i\perp} \\ E_{i\parallel} \end{bmatrix}, \quad \begin{bmatrix} E_{t+} \\ E_{t-} \end{bmatrix} = \begin{bmatrix} T_{++} & T_{+-} \\ T_{-+} & T_{--} \end{bmatrix} \begin{bmatrix} E_{i+} \\ E_{i-} \end{bmatrix}, \tag{30}$$

where

$$R_{11} = \frac{(Z_c^2 - Z_0^2)\cos\theta(\cos\theta_+ + \cos\theta_-) + 2Z_0Z_c(\cos^2\theta - \cos\theta_+\cos\theta_-)}{\Delta}, \tag{31}$$

$$R_{12} = \frac{i2Z_0Z_c\cos\theta(\cos\theta_+ - \cos\theta_-)}{\Delta}, \tag{32}$$

$$R_{21} = \frac{-i2Z_0Z_c\cos\theta(\cos\theta_+ - \cos\theta_-)}{\Delta}, \tag{33}$$

$$R_{22} = \frac{-(Z_c^2 - Z_0^2)\cos\theta(\cos\theta_+ + \cos\theta_-) + 2Z_0Z_c(\cos^2\theta - \cos\theta_+\cos\theta_-)}{\Delta}, \tag{34}$$

$$T_{++} = \frac{2Z_c(Z_c + Z_0)\cos\theta(\cos\theta + \cos\theta_-)}{\Delta}, \tag{35}$$

$$T_{+-} = \frac{-2Z_c(Z_c - Z_0)\cos\theta(\cos\theta - \cos\theta_-)}{\Delta}, \tag{36}$$

$$T_{-+} = \frac{-2Z_c(Z_c - Z_0)\cos\theta(\cos\theta - \cos\theta_+)}{\Delta}, \tag{37}$$

$$T_{--} = \frac{2Z_c(Z_c + Z_0)\cos\theta(\cos\theta + \cos\theta_+)}{\Delta}, \tag{38}$$

$$\Delta = (Z_c^2 + Z_0^2)\cos\theta(\cos\theta_+ + \cos\theta_-) + 2Z_0Z_c(\cos^2\theta + \cos\theta_+\cos\theta_-), \tag{39}$$

$$E_{i\pm} = \frac{E_{i\perp} \mp iE_{i\parallel}}{2}. \tag{40}$$

4. No-reflection conditions for chiral media

We find from Eqs. (30)-(34) that the relation between the electric field of the incident wave and that of the reflected wave is written as (Tamayama et al., 2008)

$$\begin{bmatrix} E_{r\perp} \\ E_{r\parallel} \end{bmatrix} = \frac{1}{\Delta}M_R \begin{bmatrix} E_{i\perp} \\ E_{i\parallel} \end{bmatrix}, \quad M_R = c_u I + c_2\sigma_2 + c_3\sigma_3, \tag{41}$$

$$c_u = 2Z_0Z_c(\cos^2\theta - \cos\theta_+\cos\theta_-), \tag{42}$$

$$c_2 = -2Z_0Z_c\cos\theta(\cos\theta_+ - \cos\theta_-), \tag{43}$$

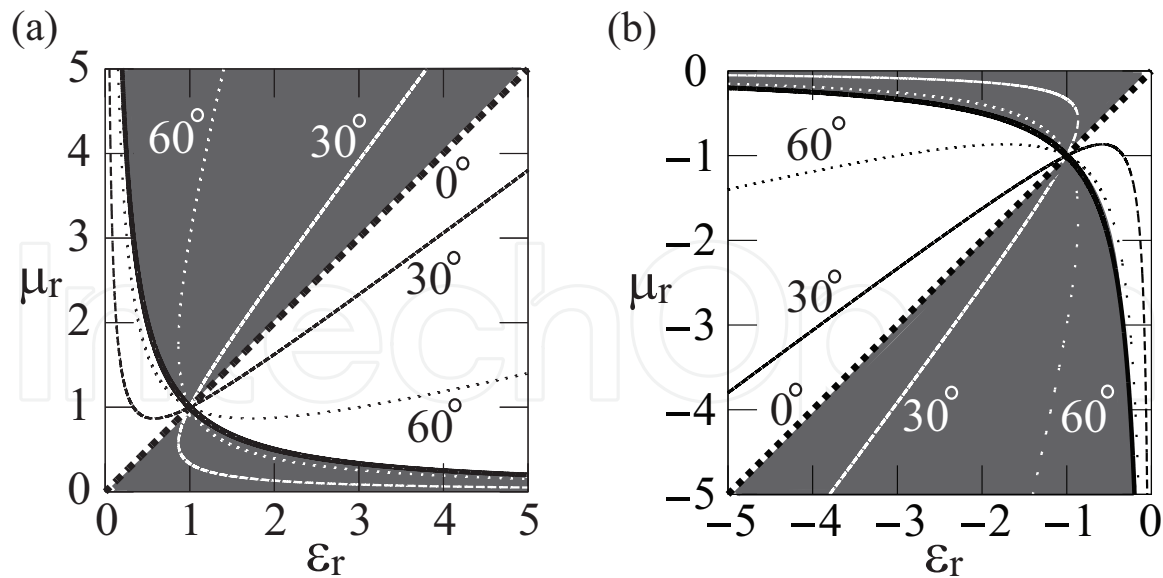$$c_3 = (Z_c^2 - Z_0^2)\cos\theta(\cos\theta_+ + \cos\theta_-), \tag{44}$$

Fig. 2. Contour lines of no-reflection angles for TM and TE waves (a) in first quadrant and (b) in third quadrant of (ε_r, μ_r)-plane. No-reflection condition exists for TM (TE) waves in white (gray) region.

where we introduce the unit matrix I and the Pauli matrices (Sakurai, 1994):

$$\sigma_2 = \begin{bmatrix} 0 & -i \\ i & 0 \end{bmatrix}, \quad \sigma_3 = \begin{bmatrix} 1 & 0 \\ 0 & -1 \end{bmatrix}. \tag{45}$$

The reflection matrix M_R can be rewritten as

$$M_R = c_u I + c_\varphi \sigma_\varphi, \tag{46}$$

where $c_\varphi = \sqrt{c_2^2 + c_3^2}$, $\sigma_\varphi = \sigma_2 \sin \varphi + \sigma_3 \cos \varphi$, $\sin \varphi = c_2 / c_\varphi$, and $\cos \varphi = c_3 / c_\varphi$.

The no-reflection condition is satisfied when M_R has at least one vanishing eigenvalue, namely, $\det(M_R) = 0$ or $\operatorname{rank}(M_R) \leq 1$. For the incident wave with the corresponding eigenpolarization, the reflection is nullified. From Eq. (46), we observe that the eigenvalue problem for M_R is reduced to that for σ_φ. The eigenvalues of σ_φ are ± 1, and their corresponding eigenpolarizations are $e_{\varphi+} = \cos(\varphi/2) e_z + i \sin(\varphi/2)(e_x \sin\theta + e_y \cos\theta)$ and $e_{\varphi-} = \sin(\varphi/2) e_z - i \cos(\varphi/2)(e_x \sin\theta + e_y \cos\theta)$. Therefore, M_R has one vanishing eigenvalue when $c_u = c_\varphi \neq 0$ ($c_u = -c_\varphi \neq 0$) is satisfied, and no-reflection is achieved for the incident wave with polarization $e_{\varphi-}$ ($e_{\varphi+}$). When $c_u = c_\varphi = 0$, M_R becomes a zero matrix; no-reflection is achieved for arbitrary polarized incident waves.

4.1 In case of $\zeta = 0$ (achiral media)

The reflection matrix is written as $M_R = c_u I + c_3 \sigma_3$. The eigenpolarizations are $e_x \sin\theta + e_y \cos\theta$ and e_z; therefore, the no-reflection condition can only be satisfied for linearly polarized waves. The no-reflection effect is observed at a particular incident angle that satisfies $c_u = \pm c_3$. The condition $c_u = c_3$ ($c_u = -c_3$) yields a no-reflection angle, called the Brewster angle, for TM (TE) waves in isotropic achiral media.

From $c_u = \pm c_3$, the no-reflection angles θ_{TM} and θ_{TE} for TM and TE waves are derived as follows:

$$\theta_{TM} = \arcsin\sqrt{\frac{\varepsilon_r^2 - \varepsilon_r \mu_r}{\varepsilon_r^2 - 1}}, \quad \theta_{TE} = \arcsin\sqrt{\frac{\mu_r^2 - \varepsilon_r \mu_r}{\mu_r^2 - 1}}, \tag{47}$$

where $\varepsilon_r = \varepsilon/\varepsilon_0$ is the relative permittivity and $\mu_r = \mu/\mu_0$ is the relative permeability. Figure 2 shows the contour lines of the no-reflection angles. The no-reflection effect can be observed for TM (TE) waves in the white (gray) region. The no-reflection condition exists in the whole region of the first and third quadrants of the (ε_r, μ_r)-plane except $\varepsilon_r = \mu_r^{-1} \neq \pm 1$. The intersection of the contour lines of the no-reflection angles in the first quadrant of the (ε_r, μ_r)-plane corresponds to a vacuum $(\varepsilon_r, \mu_r) = (1,1)$ and that in the third quadrant corresponds to an anti-vacuum $(\varepsilon_r, \mu_r) = (-1,-1)$. For the medium with parameters that correspond to these intersections, M_R becomes a zero matrix for any incident angle; arbitrary polarized waves are not reflected for all angles of incidence.

4.2 In case of $\xi \neq 0$, $k_+ \neq -k_-$, and $Z_c \neq Z_0$ (impedance unmatched chiral media)

The conditions $\xi \neq 0$, $k_+ \neq -k_-$, and $Z_c \neq Z_0$ give $\varphi \neq n\pi/2$ with integer n. The eigenpolarizations are $e_{\varphi\pm}$; hence, the no-reflection condition can only be satisfied for elliptically polarized (EP) waves. The no-reflection effect is observed at a particular incident angle satisfying $c_u = \pm c_\varphi$, which is a natural extension of the usually observed no-reflection effect, or the Brewster effect in achiral media.

The no-reflection angles are derived from the zero eigenvalue condition $c_u = \pm c_\varphi$. The contour lines of the no-reflection angles are shown in the left panels of Fig. 3. The no-reflection condition in the case of $\xi = 0$ exists in the whole region of the first and third quadrants of the (ε_r, μ_r)-plane except $\varepsilon_r = \mu_r^{-1} \neq \pm 1$, as shown in Fig. 2, while in the case of $\xi \neq 0$, there is a region where the no-reflection condition does not exist, which is represented as the gray region in Fig. 3. In addition, the no-reflection condition also exists in the second and fourth quadrants, which correspond to strong chiral media ($k_+ k_- < 0$). The right panels of Fig. 3 show the incident polarization for which the no-reflection condition is satisfied. The polarization is described in terms of the ellipticity $\alpha = \arctan(E_\parallel/iE_\perp)$. The condition $\alpha > 0$ ($\alpha < 0$) denotes left (right) elliptically polarized wave and $|\alpha| = 90°$ ($|\alpha| = 0$) corresponds to TM (TE) wave. When $|\alpha| > 45°$ ($|\alpha| < 45°$), the major axis of the polarization ellipse is perpendicular (parallel) to e_z and the minor axis is parallel (perpendicular) to e_z, namely, the no-reflection condition is satisfied for TM-like (TE-like) EP waves.

4.3 In case of $\xi \neq 0$, $k_+ \neq -k_-$, and $Z_c = Z_0$ (impedance matched chiral media)

The reflection matrix becomes $M_R = c_u I + c_2 \sigma_2$. The eigenpolarizations are $[e_z \pm i(e_x \sin\theta + e_y \cos\theta)]/\sqrt{2}$; hence, the no-reflection condition can only be satisfied for CP waves. The condition $\cos\theta_+ = \cos\theta$ ($\cos\theta_- = \cos\theta$) is required to satisfy $c_u = -c_2$ ($c_u = c_2$), which is the no-reflection condition for LCP (RCP) waves. Note that once $|k_+| = k_0$ ($|k_-| = k_0$) is satisfied by selecting the constants of medium, $c_u = -c_2$ ($c_u = c_2$) is satisfied for any incident angle. That is, the no-reflection condition is satisfied for all angles of incidence (Tamayama et al., 2008).

We derive the explicit relations among ε, μ, and ξ for the no-reflection condition for CP waves. From the above discussion, both $Z_c = Z_0$ and $|k_+| = k_0$ ($|k_-| = k_0$) are necessary and yield the
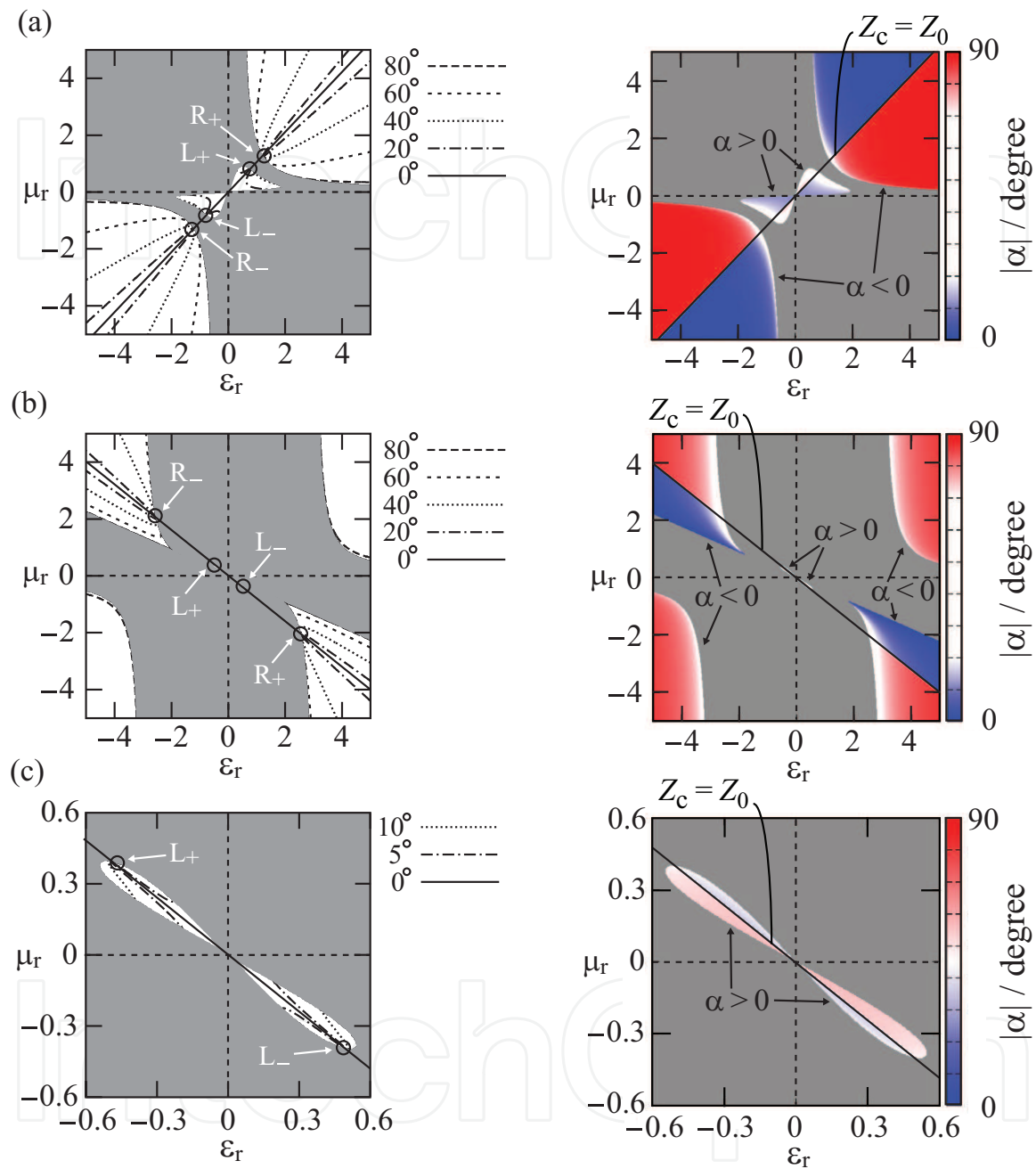
Fig. 3. No-reflection conditions (a) for $\xi_r = \xi Z_0 = 0.2$ and (b), (c) for $\xi_r = 1.5$. [Note that the scale of (c) is different from other figures.] (left panels); contour lines of no-reflection angles. L_+ and R_+ (L_- and R_-) represent the no-reflection conditions for LCP and RCP waves written in Eq. (48) [Eq. (49)], respectively. (right panels); ellipticity α of incident polarization for which no-reflection condition is satisfied. Sign of α is reversed if sign of ξ_r is reversed. No-reflection conditions do not exist in gray region.
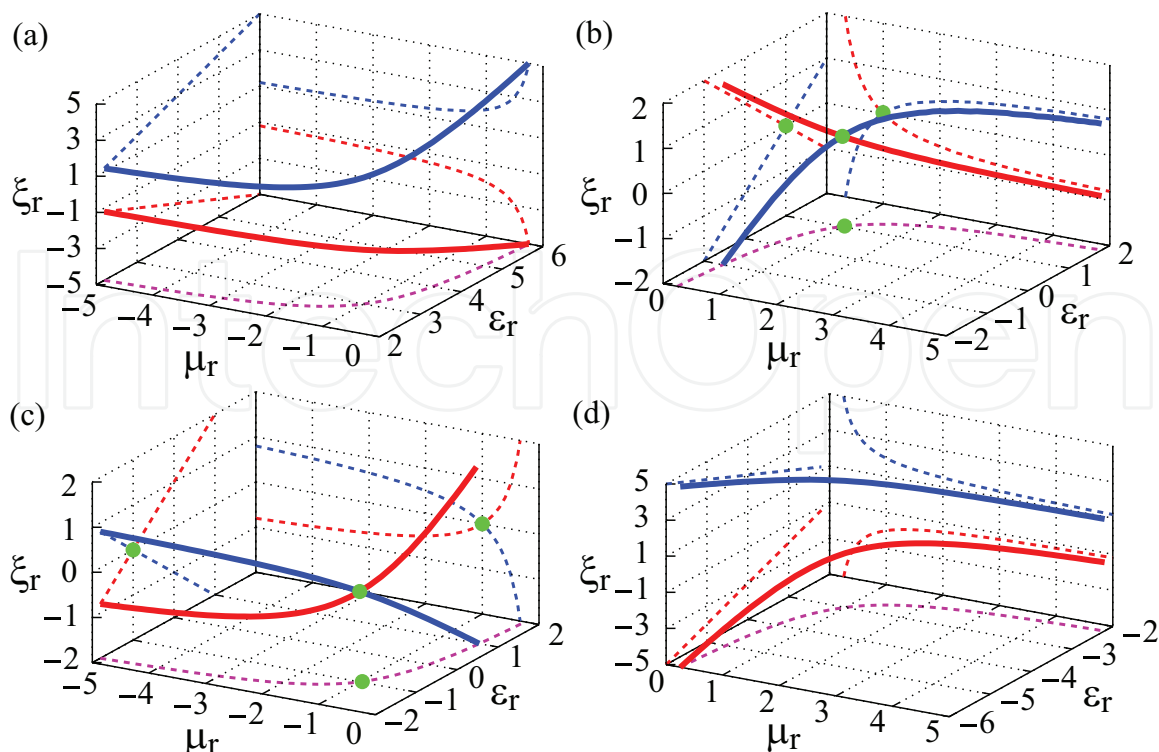
Fig. 4. Relations among ε_r, μ_r, and ξ_r that satisfy no-reflection condition for CP waves: (a), (b) relations given by Eq. (48), and (c), (d) relations given by Eq. (49). Red (blue) solid lines represent no-reflection condition for LCP (RCP) waves. Dashed lines are projections of solid lines on each plane. Green solid circles correspond to (b) vacuum and (c) anti-vacuum.

following relations:

$$\varepsilon_r = -(\pm\xi_r - 1), \quad \mu_r = \frac{\pm 1}{\xi_r \pm 1} \quad \text{(from } k_\pm = k_0\text{)}, \tag{48}$$

$$\varepsilon_r = \pm\xi_r - 1, \quad \mu_r = -\frac{\pm 1}{\xi_r \pm 1} \quad \text{(from } k_\pm = -k_0\text{)}, \tag{49}$$

where $\xi_r = \xi Z_0$ is the normalized chirality parameter. The positive (negative) sign in Eqs. (48) and (49) indicates the condition for LCP (RCP) waves. Figures 4(a) and 4(b) [4(c) and 4(d)] represent the relations among ε_r, μ_r, and ξ_r shown in Eq. (48) [Eq. (49)]. Note that the no-reflection conditions for CP waves correspond to the intersections of the contour lines of the no-reflection angles in Fig. 3. By using the electric susceptibility $\chi_e = \varepsilon_r - 1$ and magnetic susceptibility $\chi_m = 1 - \mu_r^{-1}$, Eqs. (48) and (49) are reduced to simpler forms:

$$\chi_e = \chi_m = \mp\xi_r, \tag{50}$$

$$\chi_e + 2 = \chi_m - 2 = \pm\xi_r, \tag{51}$$

respectively, where the upper (lower) sign corresponds to the condition for LCP (RCP) waves. We clarify the physical meaning of the no-reflection effect for CP waves by considering the medium polarization $\boldsymbol{P}$ and magnetization $\boldsymbol{M}$ induced by $\boldsymbol{E}$ and $\boldsymbol{B}$ in CP waves. For simplicity, assume that the no-reflection condition is satisfied for LCP waves. $\boldsymbol{P}$ and $\boldsymbol{M}$ are given by $\boldsymbol{P} = \boldsymbol{P}_E + \boldsymbol{P}_B$ and $\boldsymbol{M} = \boldsymbol{M}_B + \boldsymbol{M}_E$, where $\boldsymbol{P}_E = (\varepsilon - \varepsilon_0)\boldsymbol{E}$, $\boldsymbol{P}_B = -i\xi\boldsymbol{B}$, $\boldsymbol{M}_B = -(\mu^{-1} - \mu_0^{-1})\boldsymbol{B}$, and $\boldsymbol{M}_E = i\xi\boldsymbol{E}$ (Serdyukov et al., 2001). First, we calculate $\boldsymbol{P}$ and $\boldsymbol{M}$ when Eq. (48) is satisfied. From

the relation $H = (i/Z_c)E$ that is satisfied for LCP waves (see Table 1) and Eqs. (1) and (48), it is not difficult to confirm that $P = 0$ and $M = 0$ are satisfied regardless of the propagation direction. Due to the electromagnetic mixing attributed to ξ, the polarization P_B, which is induced by the magnetic flux density, completely cancels out the polarization P_E, which is induced by the electric field. Similarly, M_E cancels out M_B. As a result of the destructive interference of electric and magnetic responses, net polarization and magnetization vanish in the case of LCP waves in the chiral medium. This implies that the chiral medium is identical to the vacuum for LCP waves. Next, we calculate P and M when Eq. (49) is satisfied. By applying a similar procedure, we obtain $P = -2\varepsilon_0 E$ and $M = -2H$, which equal the corresponding value of the anti-vacuum. Therefore, the chiral medium behaves as an anti-vacuum for LCP waves.

4.4 In case of $k_+ = -k_-$ (chiral nihility media)

In the case of chiral nihility media ($k_+ = -k_-$) (Tretyakov et al., 2003), we obtain $M_R = c_u I + c_3 \sigma_3$, which is the same representation as that in the achiral case. The no-reflection angles for TM and TE waves are written as

$$\theta_{TM} = \arcsin\sqrt{\frac{Z_r^{-2}-1}{Z_r^{-2}-n^{-2}}}, \quad \theta_{TE} = \arcsin\sqrt{\frac{Z_r^2-1}{Z_r^2-n^{-2}}}, \quad (52)$$

respectively, where $Z_r = Z_c/Z_0$ and $n = k_+/k_0 = -k_-/k_0$. The no-reflection effect in this case resembles but is different from that in the achiral case. While the transmitted wave is a linearly polarized wave in the achiral case, LCP and RCP waves that satisfy $\theta_+ = -\theta_-$ are transmitted in this case. Equations (30) and (35)-(38) show that the intensities of the transmitted LCP and RCP waves are equal.

The medium parameters satisfying the no-reflection condition are derived from

$$(\varepsilon_r + \mu_r \xi_r^2)\mu_r = 0, \quad \mu_r/(\varepsilon_r + \mu_r \xi_r^2) = Z_r^2, \quad \mu_r \xi_r = \pm n. \quad (53)$$

The first is the condition for chiral nihility ($k_+ = -k_-$), and the second and third are the conditions for the wave impedance and wavenumber. To satisfy these equations at a particular angular frequency ω_0, the medium parameters need to be written as the following equations around ω_0:

$$\varepsilon_r = \frac{n}{Z_r}\left[f(\omega-\omega_0) - \frac{1}{f(\omega-\omega_0)}\right], \quad \mu_r = nZ_r f(\omega-\omega_0), \quad \xi_r = \pm\frac{1}{Z_r f(\omega-\omega_0)}, \quad (54)$$

where the function f satisfies $\lim_{\omega\to\omega_0} f(\omega-\omega_0) = 0$.

When $Z_r = 1$ and $n = \pm 1$, namely, $Z_c = Z_0$ and $|k_\pm| = k_0$ are satisfied, the reflection matrix M_R becomes a zero matrix. Since the conditions $Z_c = Z_0$ and $|k_\pm| = k_0$ are independent of the incident angle, M_R becomes a zero matrix for all angles of incidence; arbitrary polarized waves are not reflected for any incident angle. This phenomenon has been confirmed by numerically calculating the reflectivity when $Z_c = Z_0$ and $|k_\pm| \approx k_0$ are satisfied (Qiu et al., 2008).

We consider the physical meaning of Eq. (54) when both $Z_r = 1$ and $n = \pm 1$ are satisfied. For simplicity, suppose that $(\varepsilon_r, \mu_r, \xi_r) = [f(\omega-\omega_0) - f(\omega-\omega_0)^{-1}, f(\omega-\omega_0), f(\omega-\omega_0)^{-1}]$ are satisfied in this paragraph. The medium polarization and magnetization are found to be $P = \varepsilon_0 f(\omega-\omega_0)E \to 0$ and $M = f(\omega-\omega_0)H \to 0$ for LCP waves and $P = \varepsilon_0[f(\omega-\omega_0) - 2]E \to -2\varepsilon_0 E$ and $M = [f(\omega-\omega_0) - 2]H \to -2H$ for RCP waves when $\omega \to \omega_0$. This implies that the medium behaves as a vacuum for LCP waves and as an anti-vacuum for RCP waves.
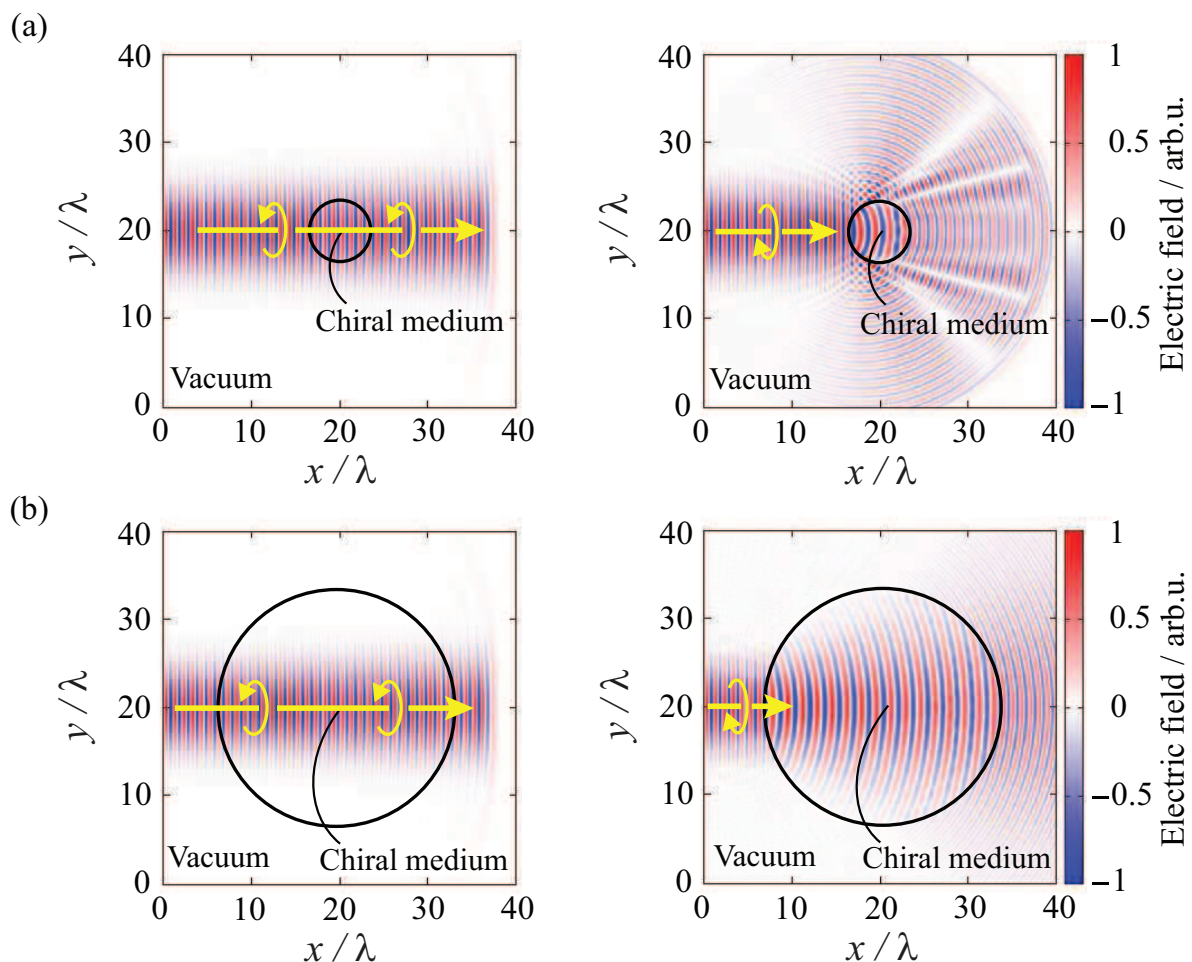
(a)

(b)

Fig. 5. Scattering of electromagnetic waves by cylindrical chiral medium when diameter of chiral medium is (a) smaller and (b) larger than beam width of electromagnetic wave. Left panels show propagations of LCP waves and right panels show those of RCP waves.

The no-reflection condition in the case of $Z_c = Z_0$ and $|k_\pm| = k_0$ can be regarded as the case of $|\xi_r| \to \infty$ in Eqs. (48) and (49). From Eqs. (48) and (49), we find that the vacuum condition for LCP (RCP) waves and the anti-vacuum condition for RCP (LCP) waves can be simultaneously satisfied when $|\xi_r| \to \infty$. In other words, the points represented by L_+ and R_- (L_- and R_+) in Fig. 3 approach each other with increasing $|\xi_r|$ and the two points become identical in the case of $|\xi_r| \to \infty$.

5. FDTD analysis of no-reflection effect for CP waves

From now, we focus on the no-reflection effect for CP waves and analyze the no-reflection effect by an FDTD method (Tamayama et al., 2008). Here, the parameters of the chiral medium are set as $\varepsilon_r = 0.75$, $\mu_r = 0.8$, and $\xi_r = 0.25$, which give $Z_c = Z_0$, $k_+ = k_0$, and $k_- = 0.6k_0$. That is, the no-reflection condition (vacuum condition) is satisfied for LCP waves.

First, we analyze the scattering of electromagnetic waves by a cylinder made of the chiral medium. To adopt the two-dimensional FDTD method, Maxwell's equations for CP waves
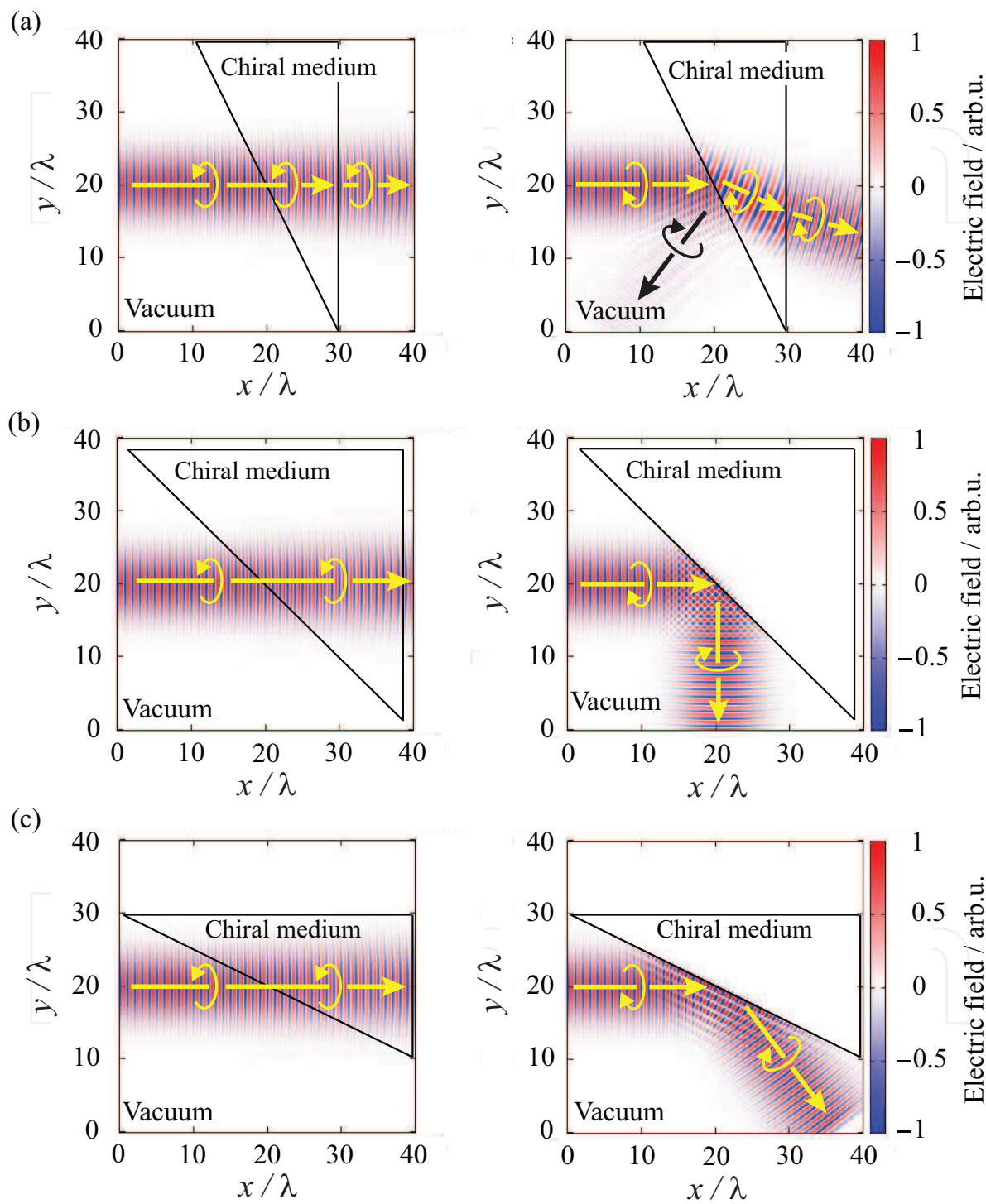
Fig. 6. Circular polarizing beam splitter. Incident angles are (a) 26.5°, (b) 45°, and (c) 63.5°. (left panels) Propagations of LCP waves and (right panels) of RCP waves.

are rearranged as follows:

$$\frac{\partial E_{z\pm}}{\partial y} = i\omega(\mu \pm \mu\xi Z_c)H_{x\pm}, \tag{55}$$

$$-\frac{\partial E_{z\pm}}{\partial x} = i\omega(\mu \pm \mu\xi Z_c)H_{y\pm}, \tag{56}$$

$$\frac{\partial H_{y\pm}}{\partial x} - \frac{\partial H_{x\pm}}{\partial y} = -i\omega\left[(\varepsilon + \mu\xi^2) \pm \frac{\mu\xi}{Z_c}\right]E_{z\pm}, \tag{57}$$

where the relation $\boldsymbol{H} = \pm(i/Z_c)\boldsymbol{E}$ is used and the positive (negative) sign corresponds to LCP (RCP) waves. Section 4.3 and Eqs. (30) and (35)-(38) show that the incident CP wave is not converted into the other CP wave on the reflection and refraction because the wave impedance matching condition $Z_c = Z_0$ is satisfied in this case. Thus, we may separately analyze the propagations of LCP and RCP waves. Figure 5 shows the propagations of electromagnetic waves when the diameter of the cylindrical chiral medium is smaller and larger than the beam width of the electromagnetic waves. One sees that LCP waves propagate with no scattering, and RCP waves are largely scattered.

Next, we analyze the propagation of electromagnetic waves when they are incident on a triangular prism made of the chiral medium. For $k_- = 0.6k_0$, Snell's equation for RCP waves is expressed as $\sin\theta = 0.6\sin\theta_-$; hence, the critical angle for RCP waves is $\theta_c = \arcsin(0.6) \simeq 37°$. Therefore, LCP waves are completely transmitted without any reflection, while RCP waves are totally reflected with the incident angle greater than $37°$. This implies that we can divide the incident waves into LCP and RCP waves. That is, the prism can be utilized as a circular polarizing beam splitter. The left (right) panels of Fig. 6 show the propagations of LCP (RCP) waves. Simulations are performed for three incident angles: $26.5°$, $45°$, and $63.5°$. The LCP wave is transmitted straight through the chiral medium without reflection for any incident angle. Although the RCP wave is partially reflected and partially transmitted in the case of $\theta < \theta_c$, it is totally reflected at the surface of the chiral medium when $\theta > \theta_c$. This result confirms that the incident wave can be split into LCP and RCP waves, and the circular polarizing beam splitter is achieved when the incident angle exceeds θ_c.

6. Conclusion

We studied the no-reflection conditions for a planar boundary between a vacuum and a chiral medium. The comparison of the no-reflection conditions for achiral and chiral media is shown in Table 2. While the no-reflection effect arises for TM and TE waves in the case of achiral media ($\xi = 0$), it arises for EP waves in the case of chiral media ($\xi \neq 0$) whose wave impedances do not equal the vacuum wave impedance. These no-reflection conditions are satisfied for a particular incident angle. When the wave impedance and the absolute value of the wavenumber in the chiral medium equal those in the vacuum for one of the CP waves, the corresponding CP wave is transmitted with no-reflection for all angles of incidence. Although the no-reflection effect for chiral nihility media resembles that for achiral media, the two cases of the no-reflection effect are different from each other in the transmitted waves.

We analyzed the no-reflection effect for CP waves by an FDTD method. The simulation results showed that a chiral medium, whose medium parameters satisfy the no-reflection effect for one of the CP waves, does not scatter the corresponding CP wave and it largely scatters the other CP wave. The FDTD simulation also demonstrated that a circular polarizing beam splitter can be achieved by a triangular prism made of the chiral medium.

$\xi = 0$

Wave impedance	$Z_c \neq Z_0$		Z_c
Medium parameters, Incident angle	$c_u = c_3$	$c_u = -c_3$	$k \equiv k$
Polarization	TM	TE	
No-reflection angle	$^\exists\theta$	$^\exists\theta$	
Refraction	yes	yes	no (wh yes (wh

$\xi \neq 0$

Wave impedance	$Z_c \neq Z_0$		Z_c
Medium parameters, Incident angle	$c_u = c_\varphi, Z_c > Z_0$ or $c_u = -c_\varphi, Z_c < Z_0$	$c_u = -c_\varphi, Z_c > Z_0$ or $c_u = c_\varphi, Z_c < Z_0$	$k_+ = \pm k_0$
Polarization	TM-like EP	TE-like EP	LCP
No-reflection angle	$^\exists\theta$	$^\exists\theta$	$^\forall\theta$
Refraction	yes	yes	no (when $k_+ = k_0$) yes (when $k_+ = -k_0$)

Table 2. Classification of no-reflection conditions for achiral ($\xi = 0$) and chiral ($\xi \neq 0$) media.

For future studies, we must prepare metamaterials whose ε_{r}, μ_{r}, and ζ_{r} satisfy the no-reflection conditions for EP and CP waves. Such metamaterials can be realized by employing chiral structures (Kuwata-Gonokami et al., 2005; Zhang et al., 2009; Rockstuhl et al., 2009; Wang et al., 2009) and by electromagnetically induced chirality in atomic systems (Sautenkov et al., 2005; Kästel et al., 2007).

7. Acknowledgments

8. References

Bassiri, S., Papas, C. H. & Engheta, N. (1988). Electromagnetic wave propagation through a dielectric-chiral interface and through a chiral slab, *J. Opt. Soc. Am. A* 5(9): 1450–1459.

Collin, R. E. (1990). *Field Theory of Guided Waves*, 2nd edn, IEEE Press, Piscataway, NJ.

Doyle, W. T. (1980). Graphical approach to Fresnel's equations for reflection and refraction of light, *Am. J. Phys.* 48(8): 643–647.

Fu, C., Zhang, Z. M. & First, P. N. (2005). Brewster angle with a negative-index material, *Appl. Opt.* 44(18): 3716–3724.

Futterman, J. (1995). Magnetic Brewster angle, *Am. J. Phys.* 63(5): 471.

Grzegorczyk, T. M., Thomas, Z. M. & Kong, J. A. (2005). Inversion of critical angle and brewster angle in anisotropic left-handed metamaterials, *Appl. Phys. Lett.* 86(25): 251909.

Holloway, C. L., Kuester, E. F., Baker-Jarvis, J. & Kabos, P. (2003). A Double Degative (DNG) Composite Medium Composed of Magnetodielectric Spherical Particles Embedded in a Matrix, *IEEE Trans. Antennas Propag.* 51(10): 2596–2603.

Jacob, Z., Alekseyev, L. V. & Narimanov, E. (2006). Optical Hyperlens: Far-field imaging beyond the diffraction limit, *Opt. Express* 14(18): 8247–8256.

Kästel, J., Fleischhauer, M., Yelin, S. F. & Walsworth, R. L. (2007). Tunable Negative Refraction without Absorption via Electromagnetically Induced Chirality, *Phys. Rev. Lett.* 99(7): 073602.

Kuwata-Gonokami, M., Saito, N., Ino, Y., Kauranen, M., Jefimovs, K., Vallius, T., Turunen, J. & Svirko, Y. (2005). Giant Optical Activity in Quasi-Two-Dimensional Planar Nanostructures, *Phys. Rev. Lett.* 95(22): 227401.

Lagarkov, A. N. & Kissel, V. N. (2004). Near-Perfect Imaging in a Focusing System Based on a Left-Handed-Material Plate, *Phys. Rev. Lett.* 92(7): 077401.

Lakhtakia, A. (1992). General schema for the Brewster conditions, *Optik (Stuttgart)* 90(4): 184–186.

Leonhardt, U. (2006). Optical Conformal Mapping, *Science* 312(5781): 1777–1780.

Lindell, I. V., Sihvola, A. H., Tretyakov, S. A. & Viitanen, A. J. (1994). *Electromagnetic Waves in Chiral and Bi-Isotropic Media*, Artech House, Boston, MA.

Liu, Z., Lee, H., Xiong, Y., Sun, C. & Zhang, X. (2007). Far-Field Optical Hyperlens Magnifying Sub-Diffraction-Limited Objects, *Science* 315(5819): 1686.

Pendry, J. B. (2000). Negative Refraction Makes a Perfect Lens, *Phys. Rev. Lett.* 85(18): 3966–3969.

Pendry, J. B., Holden, A. J., Robbins, D. J. & Stewart, W. J. (1999). Magnetism from Conductors and Enhanced Nonlinear Phenomena, *IEEE Trans. Microwave Theory Tech.* 47(11): 2075–2084.

Pendry, J. B., Schurig, D. & Smith, D. R. (2006). Controlling Electromagnetic Fields, *Science* 312(5781): 1780–1782.

Qiu, C.-W., Burokur, N., Zouhd, S. & Li, L.-W. (2008). Chiral nihility effects on energy flow in chiral materials, *J. Opt. Soc. Am. A* 25(1): 55–63.

Rockstuhl, C., Menzel, C., Paul, T. & Lederer, F. (2009). Optical activity in chiral media composed of three-dimensional metallic meta-atoms, *Phys. Rev. B* 79(3): 035321.

Sakurai, J. J. (1994). *Modern Quantum Mechanics*, revised edn, Addison-Wesley, Reading, MA.

Saleh, B. E. A. & Teich, M. C. (2007). *Fundamentals of Photonics*, 2nd edn, Wiley-Interscience, Hoboken, NJ.

Sautenkov, V. A., Rostovtsev, Y. V., Chen, H., Hsu, P., Agarwal, G. S. & Scully, M. O. (2005). Electromagnetically Induced Magnetochiral Anisotropy in a Resonant Medium, *Phys. Rev. Lett.* 94(23): 233601.

Schurig, D., Mock, J. J., Justice, B. J., Cummer, S. A., Pendry, J. B., Starr, A. F. & Smith, D. R. (2006). Metamaterial Electromagnetic Cloak at Microwave Frequencies, *Science* 314(5801): 977–980.

Serdyukov, A., Semchenko, I., Tretyakov, S. & Sihvola, A. (2001). *Electromagnetics of Bi-anisotropic Materials: Theory and Applications*, Gordon and Breach Science Publishers, LH, Amsterdam.

Shelby, R. A., Smith, D. R. & Schultz, S. (2001). Experimental verification of a negative index of refraction, *Science* 292(5514): 77–79.

Shen, N.-H., Wang, Q., Chen, J., Fan, Y.-X., Ding, J. & Wang, H.-T. (2006). Total transmission of electromagnetic waves at interface associated with an indefinite medium, *J. Opt. Soc. Am B* 23(5): 904–912.

Shu, W., Ren, Z., Luo, H. & Li, F. (2007). Brewster angle for anisotropic materials from the extinction theorem, *Appl. Phys. A* 87(2): 297–303.

Taflove, A. & Hagness, S. C. (2005). *Computational Electrodynamics: The Finite-Difference Time-Domain Method*, 3rd edn, Artech House, Norweed, MA.

Tamayama, Y., Nakanishi, T., Sugiyama, K. & Kitano, M. (2006). Observation of Brewster's effect for transverse-electric electromagnetic waves in metamaterials: Experiment and theory, *Phys. Rev. B* 73(19): 193104.

Tamayama, Y., Nakanishi, T., Sugiyama, K. & Kitano, M. (2008). An invisible medium for circularly polarized electromagnetic waves, *Opt. Express* 16(25): 20869–20875.

Tanaka, T., Ishikawa, A. & Kawata, S. (2006). Unattenuated light transmission through the interface between two materials with different indices of refraction using magnetic metamaterials, *Phys. Rev. B* 73(12): 125423.

Tretyakov, S., Nefedov, I., Sihvola, A., Maslovski, S. & Simovsli, C. (2003). Waves and energy in chiral nihility, *J. of Electromagn. Waves and Appl.* 17(5): 695–706.

Veselago, V. G. (1968). The electrodynamics of substances with simultaneously negative values of ε and μ, *Sov. Phys. Usp.* 10(4): 509–514.

Wang, B., Zhou, J., Koschny, T. & Soukoulis, C. M. (2009). Nonplanar chiral metamaterials with negative index, *Appl. Phys. Lett.* 94(15): 151112.

Watanabe, R., Iwanaga, M. & Ishihara, T. (2008). s-polarization Brewster's angle of stratified metal-dielectric metamaterial in optical regime, *Phys. Stat. Sol. (b)* 245(12): 2696–2701.

Zhang, S., Fan, W., Malloy, K. J., Brueck, S. R. J., Panoiu, N. C. & Osgood, R. M. (2005).

Near-infrared double negative metamaterials, *Opt. Express* 13(13): 4922–4930.

Zhang, S., Park, Y.-S., Li, J., Lu, X., Zhang, W. & Zhang, X. (2009). Negative Refractive Index in Chiral Metamaterials, *Phys. Rev. Lett.* 102(2): 023901.
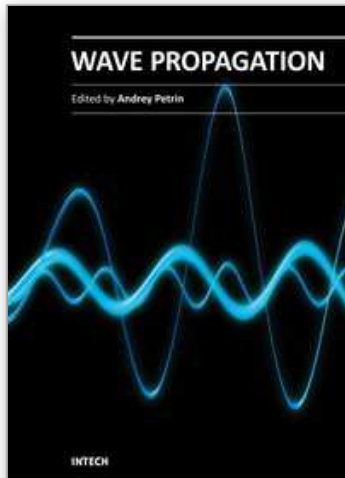
Wave Propagation

Edited by Dr. Andrey Petrin

The book collects original and innovative research studies of the experienced and actively working scientists in the field of wave propagation which produced new methods in this area of research and obtained new and important results. Every chapter of this book is the result of the authors achieved in the particular field of research. The themes of the studies vary from investigation on modern applications such as metamaterials, photonic crystals and nanofocusing of light to the traditional engineering applications of electrodynamics such as antennas, waveguides and radar investigations.

How to reference

In order to correctly reference this scholarly work, feel free to copy and paste the following:

INTECH
open science | open minds